Lawrence Berkeley National Laboratory

Recent Work

Title

LONG-PATH LASER INTERFEROMETER CELLS FOR USE IN CONDENSED PHASES. I. ELECTRODEPOSITION CELLS. ; H. INTERFEROMETIC CELLS OTHER THAN ELECTRODEPOSITION.

Permalink

https://escholarship.org/uc/item/4w7997x1

Authors

O'Brien, R.N.
Beer, E.A.
Beach, K.
et al.

Publication Date

1966-07-01

eScholarship.org Powered by the California Digital Library
University of California

UCRL-17002

University of California

Ernest O. Lawrence Radiation Laboratory

LONG-PATH LASER INTERFEROMETER CELLS
FOR USE IN CONDENSED PHASES

TWO-WEEK LOAN COPY

This is a Library Circulating Copy which may be borrowed for two weeks. For a personal retention copy, call Tech. Info. Division, Ext. 5545

Berkeley, California

DISCLAIMER

This document was prepared as an account of work sponsored by the United States Government. While this document is believed to contain correct information, neither the United States Government nor any agency thereof, nor the Regents of the University of California, nor any of their employees, makes any warranty, express or implied, or assumes any legal responsibility for the accuracy, completeness, or usefulness of any information, apparatus, product, or process disclosed, or represents that its use would not infringe privately owned rights. Reference herein to any specific commercial product, process, or service by its trade name, trademark, manufacturer, or otherwise, does not necessarily constitute or imply its endorsement, recommendation, or favoring by the United States Government or any agency thereof, or the Regents of the University of California. The views and opinions of authors expressed herein do not necessarily state or reflect those of the United States Government or any agency thereof or the Regents of the University of California.

Submitted to
Review of Scientific Instruments

UCRL-17002
Preprint

UNIVERSITY OF CALIFORNIA

Lawrence Radiation Laboratory
Berkeley, California

AEC Contract W-7405-eng-48

LONG-PATH LASER INTERFEROMETER CELLS FOR USE IN CONDENSED PHASES

I. Electrodeposition Cells

R. N. O'Brien, E. A. Beer, K. Beach and J. Leja

II. Interferometric Cells Other Than Electrodeposition

R. N. O'Brien, S. Weiner and K. S. Spiegler

July 1966

LONG-PATH LASER INTERFEROMETER CELLS FOR USE IN CONDENSED PHASES.

I. Electrodeposition Cells.

By R. N. O'Brien[1], E. A. Beer[2], K. Beach[3] and J. Leja[4]

The development of a truly long path interferometer for use in condensed phases was not possible until the uniphase out-put continuous C.W. gas laser became commercially available, although an interferometer with a path length limited by the spacial coherence of the light source (sodium vapor) but still quite long (the order of interference being limited to about 10^4) has been reported in this journal[1] and considerable work was done with it[2] and its prototypes. The spacial coherence of the laser is such that no appreciable attenuation of the intensity of a beam occurs in less than about one kilometer and the monochromisity is so good that using the Rayliegh criterion for distinguishing between fringes, cells 50-60 meters thick using water or non absorbing aqueous solutions are theoretically possible. Using previous light sources, at the very least one collimating lens was needed (sometimes a filter) the cell thickness was limited to about 5 mm and

if photography was the recording means, normal speed motion picture photography was difficult because of low light intensities, whether transmitted or reflected. Using a Spectro-Physics Model 130 gas laser with a beam expanding telescope in which the beam was expanded from 1.2 mm in diameter to as much as 60 mm in diameter fine-grained film of ASA speeds of 50-80 could be used at 8-16 frames/sec.

The theory of interferometry including methods of calculating results has been previously explained[1] and an excellent text exists[2], but briefly the formula $2\mu t \cos\varphi = n\lambda$ where μ = refractive index, t = thickness of the cell in cms, φ = the angle of incidence of light and $\cos\varphi = 1$ for all cases here considered, n = order of interference and λ = wave length of the light in cms states that along any interference fringe (n is a constant) the product of the refractive index and the path-length difference ($2\mu t$ in wedge interferometers) is a constant. If the interferometer is a rigid wedge so that t is constant at any point then when the refractive index changes the fringe must move up or down the wedge, or become curved in one direction or the other depending on the intensity and extent of the refractive index perturbation. The interference fringe in the family of cells to be considered is then a refractive index contour. All cells are of the transmission, rather than reflection type as seen in Figure I, a schematic light

path diagram. Refractive index can be related to chemical composition by the expression $\mu = KM$ where M = molarity and K is a proportionality constant that generally has an undetectable variation with concentration up to about half molar concentrations, depending on the solution. In electrolytes the foregoing is true for 1:1 electrolytes but variations of ±0.1% occur for 2:2 or any electrolyte containing highly charged or ion-pair forming species.

The refractive index can also be affected by changes in density as seen in the Lorentz-Lorenz Law

$$R = \frac{M}{P}\left(\frac{\mu^2 - 1}{\mu^2 + 2}\right)$$

where R is the molar refraction, M the molecular weight, P the density and μ the refractive index. Changes in density may occur because of changes in temperature and pressure or hydrodynamic shear. The concentration change contour (which if the solute has a density different from the solvent is also a density contour) has been utilized in electrodeposition and the cells evolved will be described here, the density change contour and the cells to study it will be described in Paper II.

An Electrochemical Interferometric Cell with Reference Electrodes

Previous cells[1,3] have had no reference electrodes, and theoretically this is a grave limitation. One cell used for non-interferometric work[4] did use a copper probe electrode and some interferometric work was done with a similar cell.[5] The cell is sealed by tightening the three clamping screws. The screws are adjusted after sealing the cell to give the desired wedge angle which is about two minutes of arc to give 3-4 fringes/mm. The first reflecting coating interface encountered (Figure I) was 90% reflecting and the second 70% so that although the cell is a multiple beam interferometer, the effective number of traverses of the cell is about 2. This avoids the problem of bending of the light rays as they traverse a region of constantly changing refractive index which causes the successive contribution to a multiple-beam fringe not to coincide in space with resultant loss of resolution.[6] The present cell as can be seen in Figure II has luggin capillaries of fine teflon tubing placed directly in front of the working surface of the electrode. The extra set of holes was used to introduce the electrolyte (Figure II b). Figure II c shows the cell set up for electrolysis and fringes showing in the cell gap. Figure III is a series of interferogram taken with this cell when the electrodes were high purity zinc and the electrolyte was 0.1N $ZnSO_4$, pH 4.5, current density 0.5 ma/cm^2.

Flowing Electrolyte Electrolysis Cell

Electrolytic processes in which stirring or forced convection is employed and particularly electro-machining where the electrolyte is pumped through the machining site, cannot be studied conveniently interfero-metrically unless the electrolyte flows into and through the cell in a hydrodynamically acceptable way. One such way is delivery from a uniform cross-section, straight, smooth channel into the space between the electrodes which must be accomplished with no sudden changes of shape, cross-sectional area or direction of flow. This cell was designed specifically to introduce at appropriate Reynolds numbers a turbulence-free stream of electrolyte. The square channels which lead the electrolyte in and out are made of teflon pieces held together with stainless steel pins. Figure IV shows the cell detail. The cell is sealed by axial pressure on the teflon cylinder by the adjustable brass ring which presses the teflon cell wall against the glass flats. The wedge angle is adjusted by the clamping screws. The cell is to be used to investigate the system $Cu/CuSO_4/Cu$ under forced convection conditions.

Rotating Disc Electrode Cell

In this modification the basic cell was fitted with a bottom electrode which protruded into the cell far enough

to fit into a hole in the bottom of a hollow cylinder of teflon (Figure V). The cylinder was shaped so that with the bottom electrode inserted into the cylinder's bottom hole it was held upright. Slices were now cut from opposite walls, the slices being thick enough to cut through the cylinder walls, to form parallel chords of the cylinder's internal diameter. A 1/8" diameter hole at the top was used to fill the cell and to admit the rotating disc electrode. When the electrode rotated within the cylinder. The coated glass flats fitted tightly to the sliced off side of the vertical cylinder and the laser light traversed the cell through the open sides of the cylinder. The cylinder served the purpose of constraining the horizontal hydrodynamic path of the electrolyte to a close approximation to a circle. It was hoped that the change of tangential velocity where the teflon cylinder walls ended and the glass began would be small enough to be neglected. The cell was 1 cm thick and the disc 3.189 mm in diameter. Figure VI (d) shows that at 300 rpm the hydrodynamic shear zone extends to about 0.38 mm as seen by the limit of the fringe perturbations. Knowing the wedge apex was downward the change in refraction index can be interpreted as a decrease in density or a dilation from the Lorentz-Lorenz expression. The other frames of Figure VI (a,b,c) show a 1 mA/cm^2 current density with no rotation in (a), in (b) the rotation has begun and the diffusion layer (which is about one half as thick as the hydrodynamic layer in (d)) has almost disappeared, in (c) a hydrodynamic shear layer is beginning to appear with a refractive index change opposite in sign to the electrochemical diffusion layer. Since a small fraction

of a fringe shift (±1/10) can be detected and the order of interference is about 4×10^4 a change in density or volume can be measured of about 1 part in 4×10^5. The possibility of using this cell as a sensitive dilatometer is being pursued.

Dropping Mercury Electrode Cell

This cell differs only in that sufficient space was provided to allow the complete electrode assembly, that is the capillary, salt bridge and degassing tube to be inserted into it. For this purpose three large holes (the largest 4.5 mm diameter) were cut in the top of the cell and the assembly inserted (Figure VII).

The cell was sealed in the usual way. The wedge angle used was about double the 2 minute of arc usually used to give more fringes, so that a full sized drop would have 4-5 fringes across its diameter. Figure VIII is a interferogram taken with a 35 mm motion picture camera under the following conditions: room temperature, drop time $1\frac{1}{4}$ seconds, -0.45 volts 0.1N $Pb(NO_3)_2$ in 1N KCl solution.

The concentration is about 2 orders of magnitude greater than that usually used, -0.45 volts vs the normal hydrogen electrode is just at the beginning of the normal polarographic wave for Pb^{2+}, so very little concentration change would be expected. The change in concentration is about 0.03N $Pb(NO_3)_2$.

The salt bridge containing KCl in agar gel can be seen to the right of the capillary. KCl (and possibly agar) is diffusing out of it causing severe perturbations to the fringe system.

Information resulting from the use of the cells will soon be published.

Acknowledgement

Some of this work was done at the University of Alberta, and supported by the National Research Council of Canada and the Defense Research Board of Canada on DRB Grant 5401-04 for which our thanks are due.

One of the authors (R. N. O'Brien) was a Visiting Scholar at the University of California, Berkeley and was supported by IMRD, LRL where most of the work was done under the auspices of the United States Atomic Energy Commission.

References

1. R. N. O'Brien, Rev. Sci. Instr. 35, 803 (1964).

2. S. Tolansky, An Introduction to Interferometry, Longmans Green, London (1953).

3. R. N. O'Brien and H. J. Axon, Trans. Inst. Metal Finishing 34, 41 (1957).

   R. N. O'Brien, Can. J. Chem. 35, 932 (1957).

   R. N. O'Brien and C. Rosenfield, Nature 187, 4741 (1960).

   R. N. O'Brien and C. Rosenfield, J. Phys. Chem. 67, 643 (1963).

   R. N. O'Brien, W. F. Yakymyshyn and J. Leja, J. Electrochem. Soc. 110, 820 (1963).

   R. N. O'Brien, Nature, 201, 74 (1964).

   R. N. O'Brien, J. Electrochem. Soc. 111, 1300 (1964).

   R. N. O'Brien and K. Kinoshita, J. Electrochem. Soc. 112, 951 (1965).

   R. N. O'Brien, C. A. Rosenfield, K. Kinoshita, W. F. Yakymyshyn and J. Leja, Can. J. Chem. 43, 3304 (1965).

   R. N. O'Brien, J. Electrochem. Soc. April 1966.

4. R. N. O'Brien and L. M. Mukherjee, J. Electrochem. Soc. 111, 1358 (1964).

5. Unpublished work of R. N. O'Brien and K. Kinoshita.

6. N. Ibl, Proc. 7th Meet. C.I.T.C.E. Lindau, 1955, Butterworths, London (1957).

FIGURE CAPTIONS (Paper 1)

Figure I — Schematic Light Path.

Figure IIa — Detail of the internal parts of the Electrodeposition Cell showing luggin capillaries leading to reference electrodes.

Figure IIb — Detail of the external parts of the Electrodeposition Cell.

Figure IIc — Photograph of the assembled cell with visible fringes showing the electrolyte gap at the centre of the picture.

Figure III — A series of interferograms taken using the Electrodeposition Cell. The top interferogram is at zero time, zero current, the middle is 16 seconds after the beginning of electrolysis at 0.5 mA/cm^2, in the $Zn/ZnSO_4/Zn$ system, cathode-over-anode orientation, 0.1N $ZnSO_4$ pH 5.5. The bottom is the same system after about 5 minutes of electrolysis, 15 seconds after switching off the current. In each interferogram an oval window of references fringes appears above the electrolysis chamber.

Figure IV — Flowing Electrolyte Electrolysis Cell.

Figure V — The Rotating Disc Cell.

Figure VI — The Result of Rotation of the Disc Electrode on the Diffusion Layer. Frame (a) shows a diffusion gradient in 2N NaOH, 0.1M $K_4Fe(CN)_6$ and 0.1M $K_3Fe(CN)_6$ formed by passing 1 mA/cm^2 with the disc polarized as the anode. Frame (b) is taken about $\frac{1}{2}$ second later and shows that the rapidly accelerating disc has almost lost its diffusion layer. Frame (c) taken about 1 second after (a) shows a hydrodynamic shear zone beginning, with dilation of the solution distorting the fringes in the opposite sense to the original electrochemical diffusion layer. Frame (d) was taken more than 10 seconds later and shows the stable hydrodynamic shear zone set up at about 300 rpm in this solution. All frames are from a 16 mm motion picture film taken at 12 frames/sec.

Figure VII — Detail of the Dropping Mercury Electrode Cell.

Figure VIII — Interferogram of a Mercury Drop Cathode. This frame was taken just before the drop fell, drop time $1\frac{1}{4}$ seconds, -0.45 volts, 0.1N $Pb(NO_3)_2$ in 1N KCl. Concentration change near the top of the drop is about 0.03N.

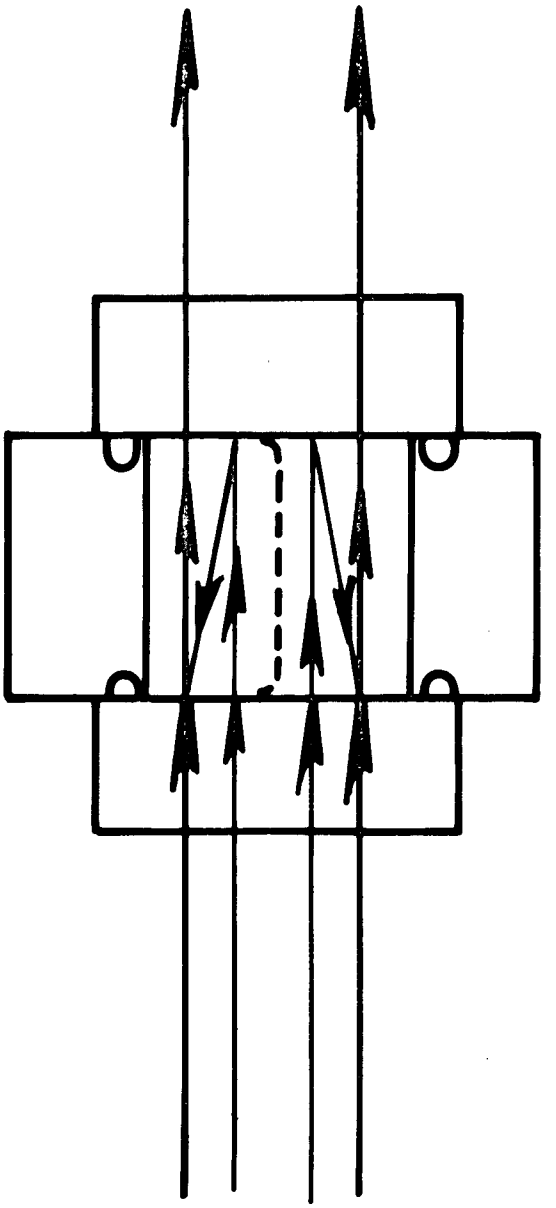

MUB-12625

Fig. I

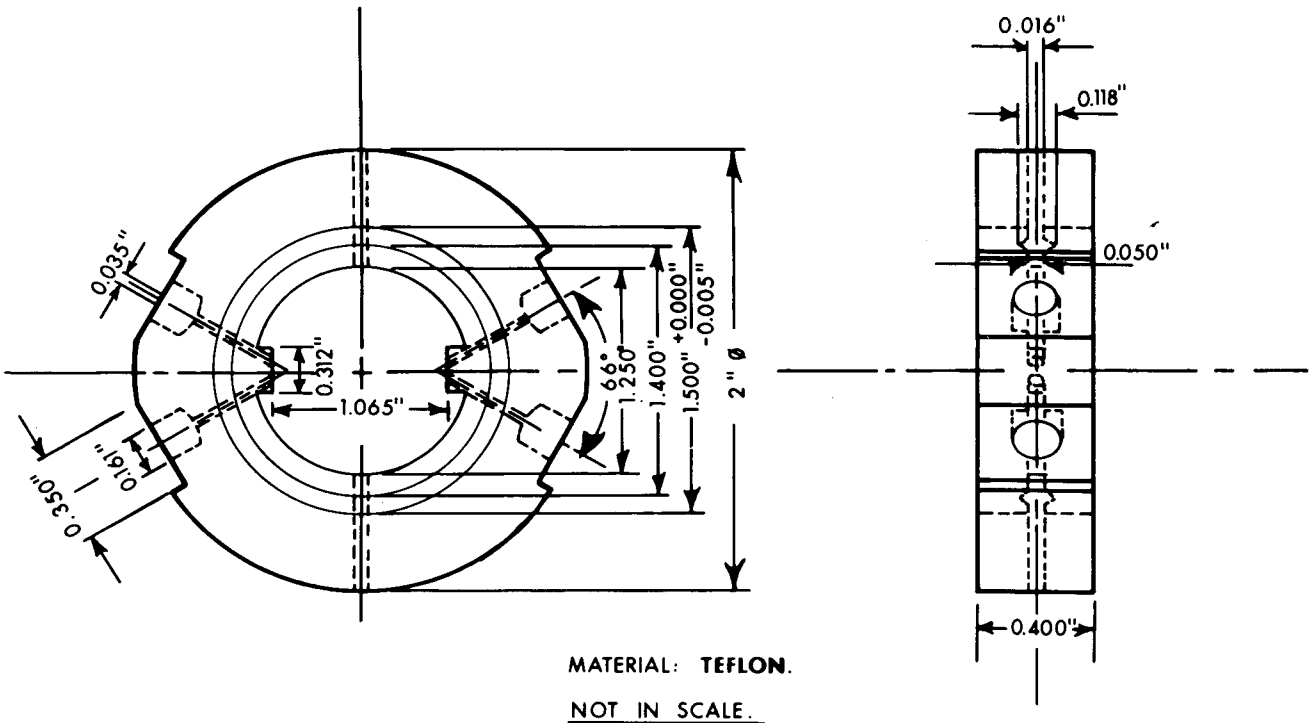

MATERIAL: **TEFLON.**

NOT IN SCALE.

THE HOLES OF 0.161" DIAMETER, HAVE A DEPTH OF APPROXIMATELY 0.125"

MUB-12626

Fig. IIa

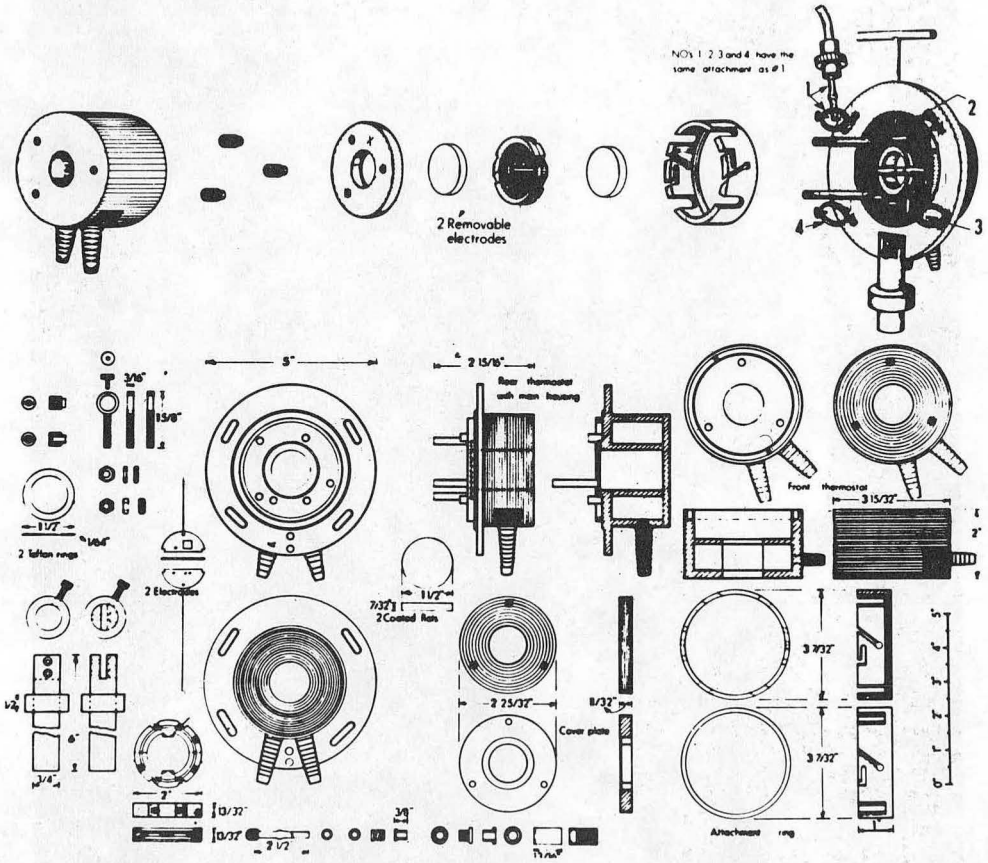

MUB-12627

Fig. IIb

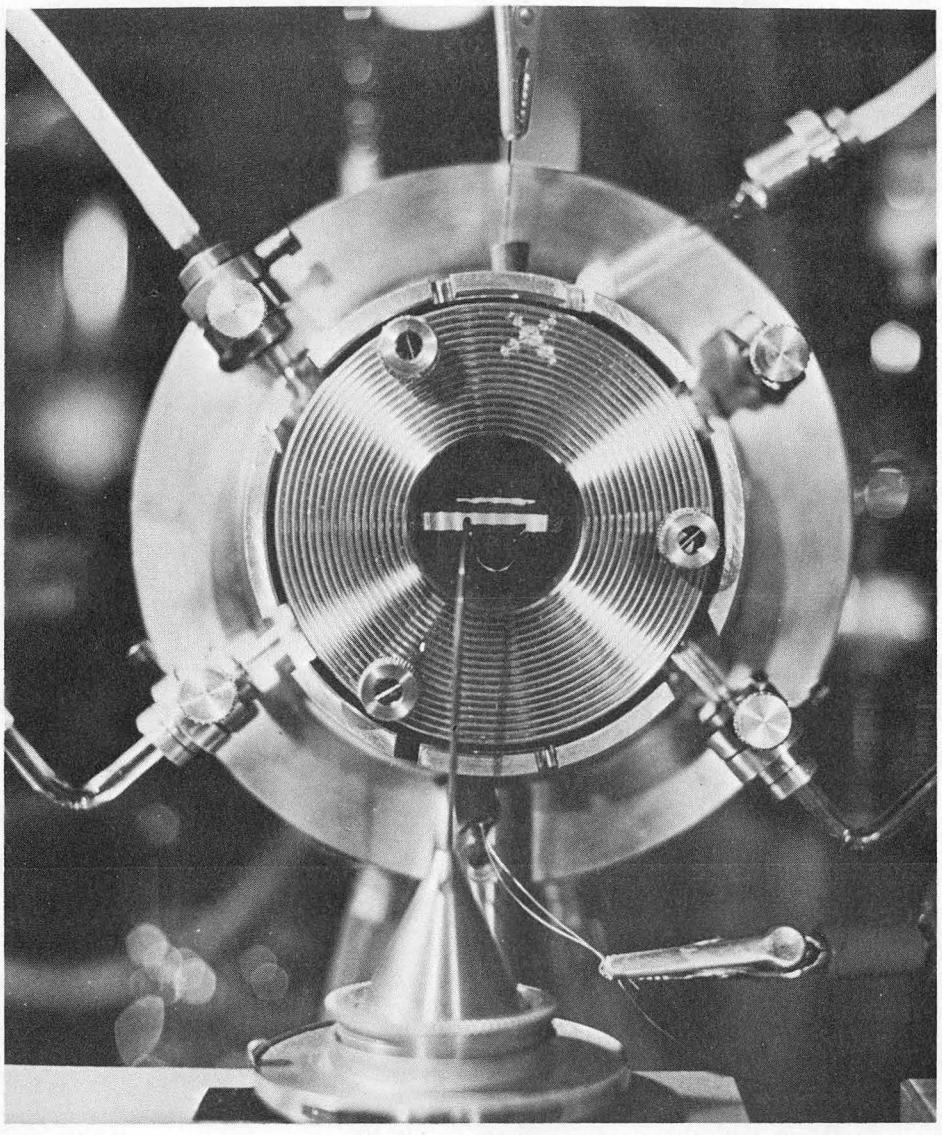

ZN-5741

Fig. IIc

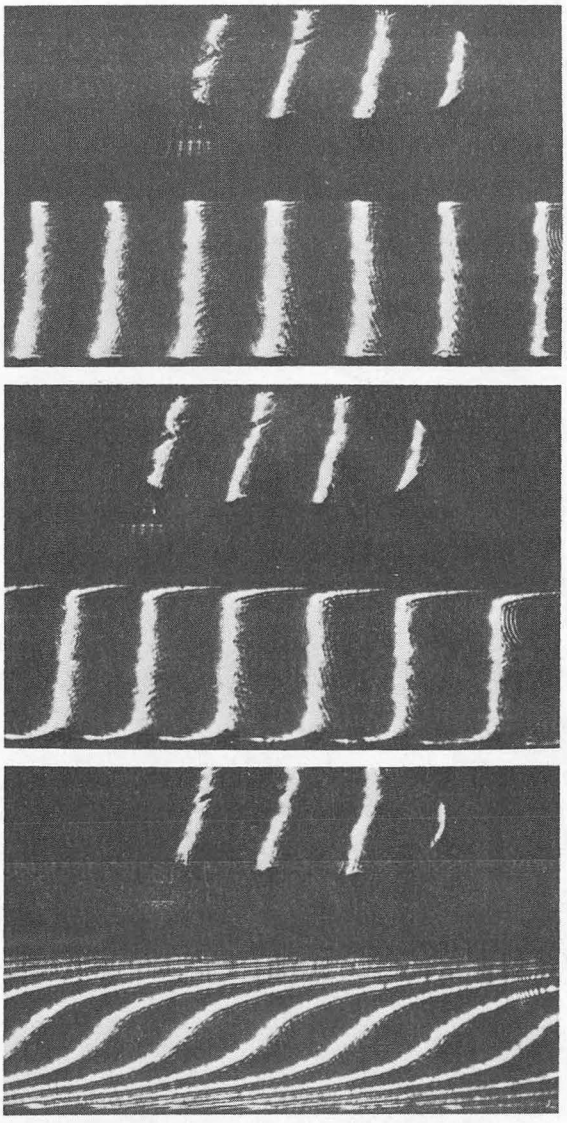

ZN - 5738

Fig. III

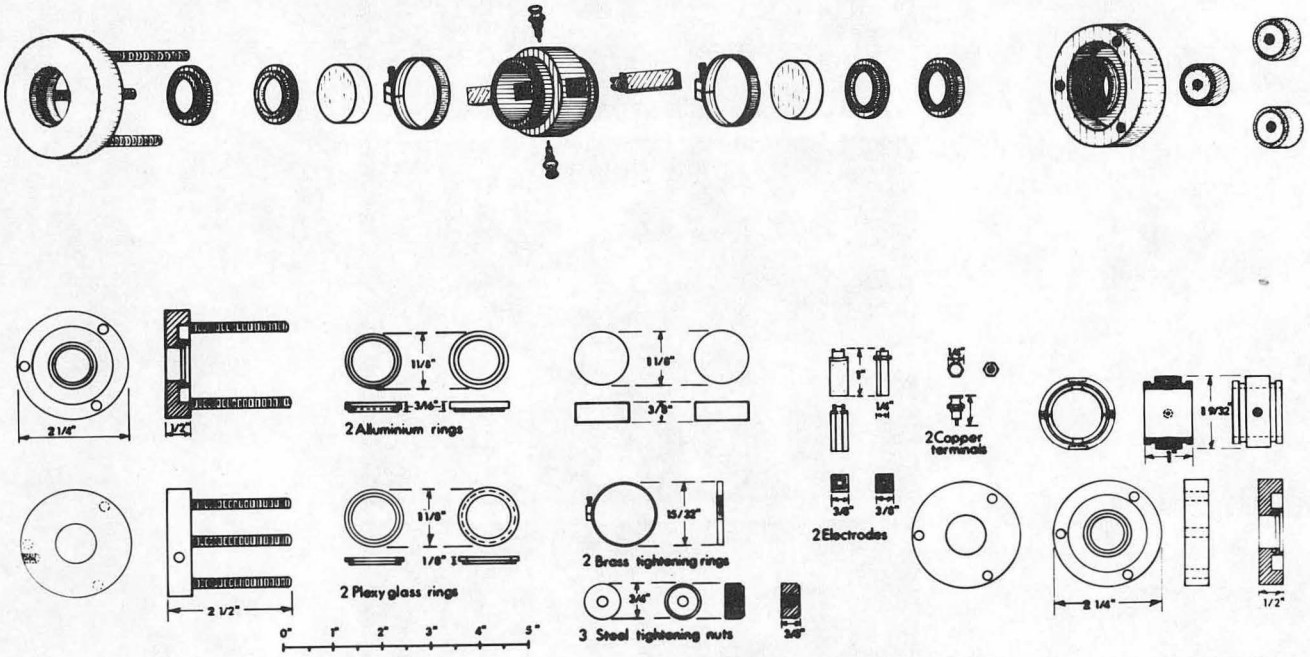

MUB-12628

Fig. IV

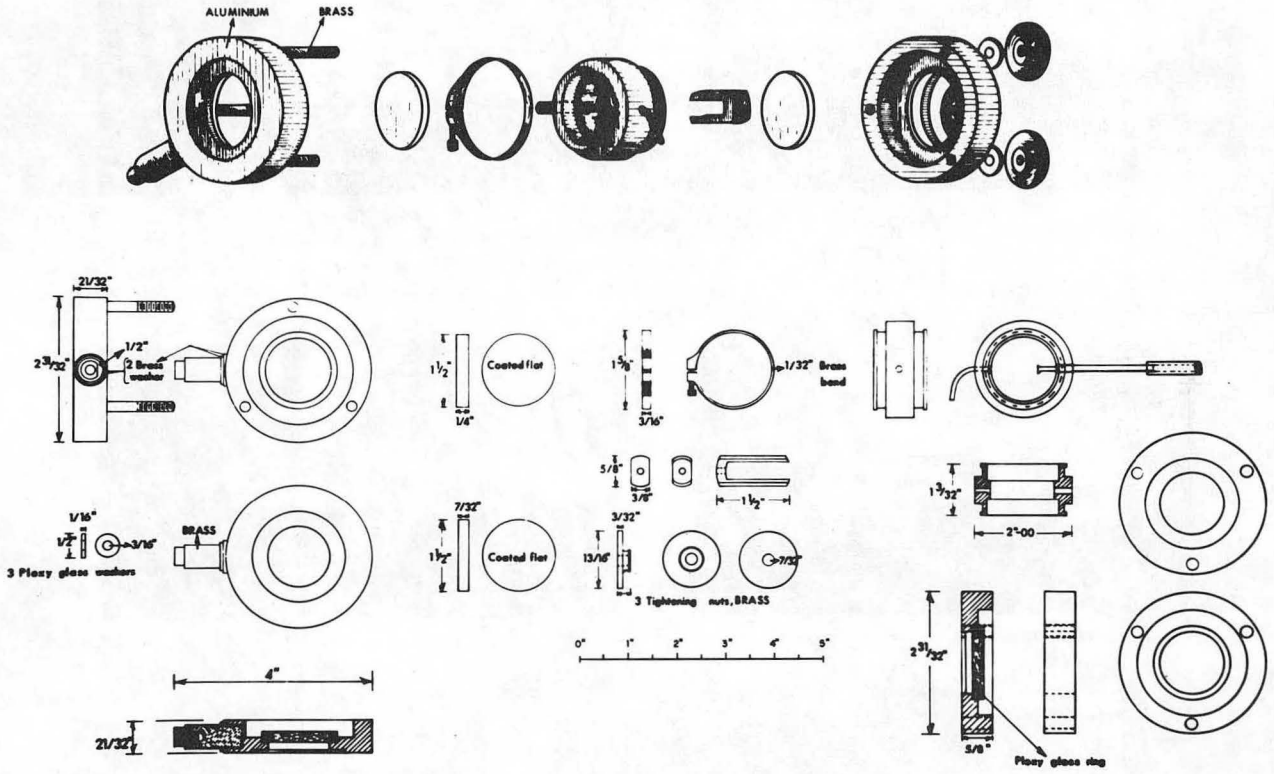

MUB-12629

Fig. V

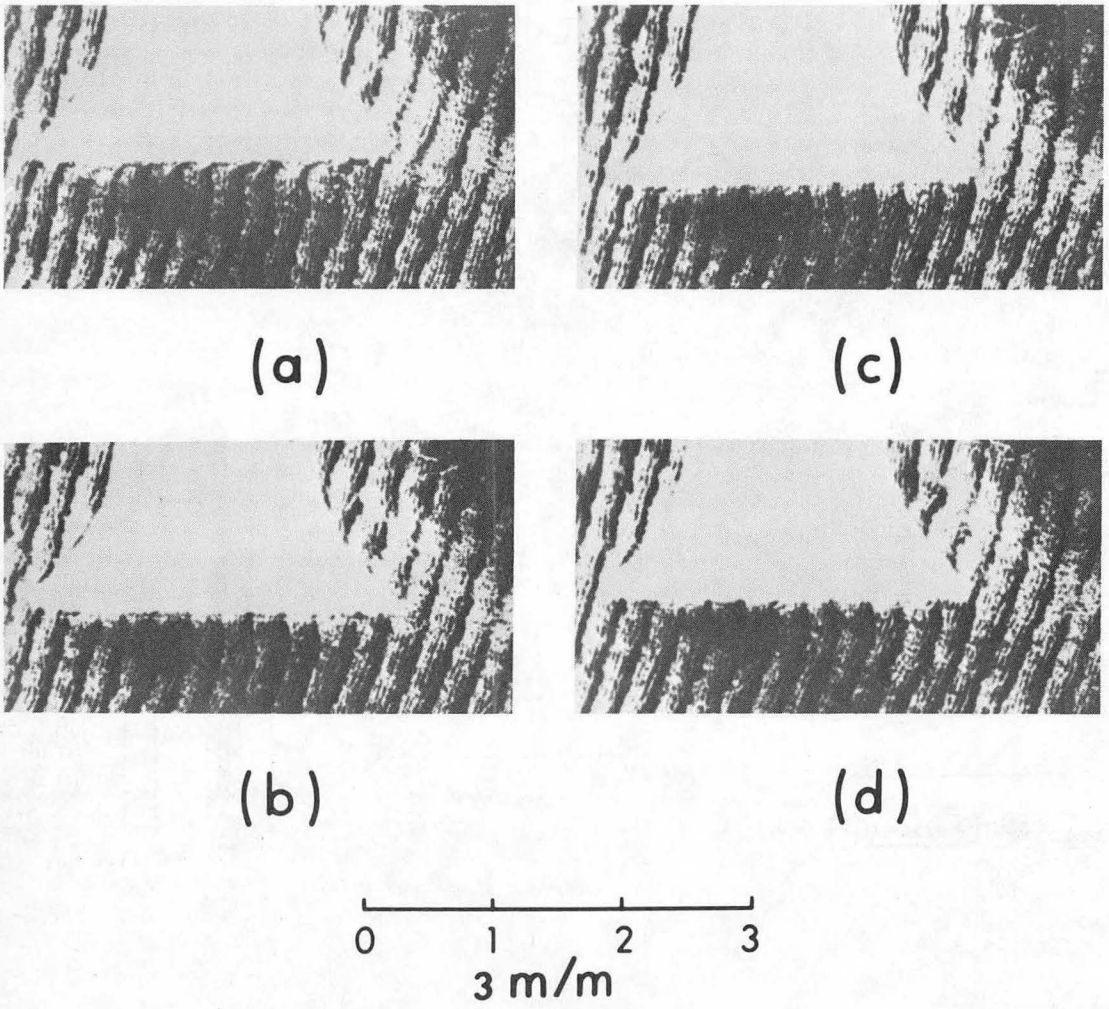

Fig. VI

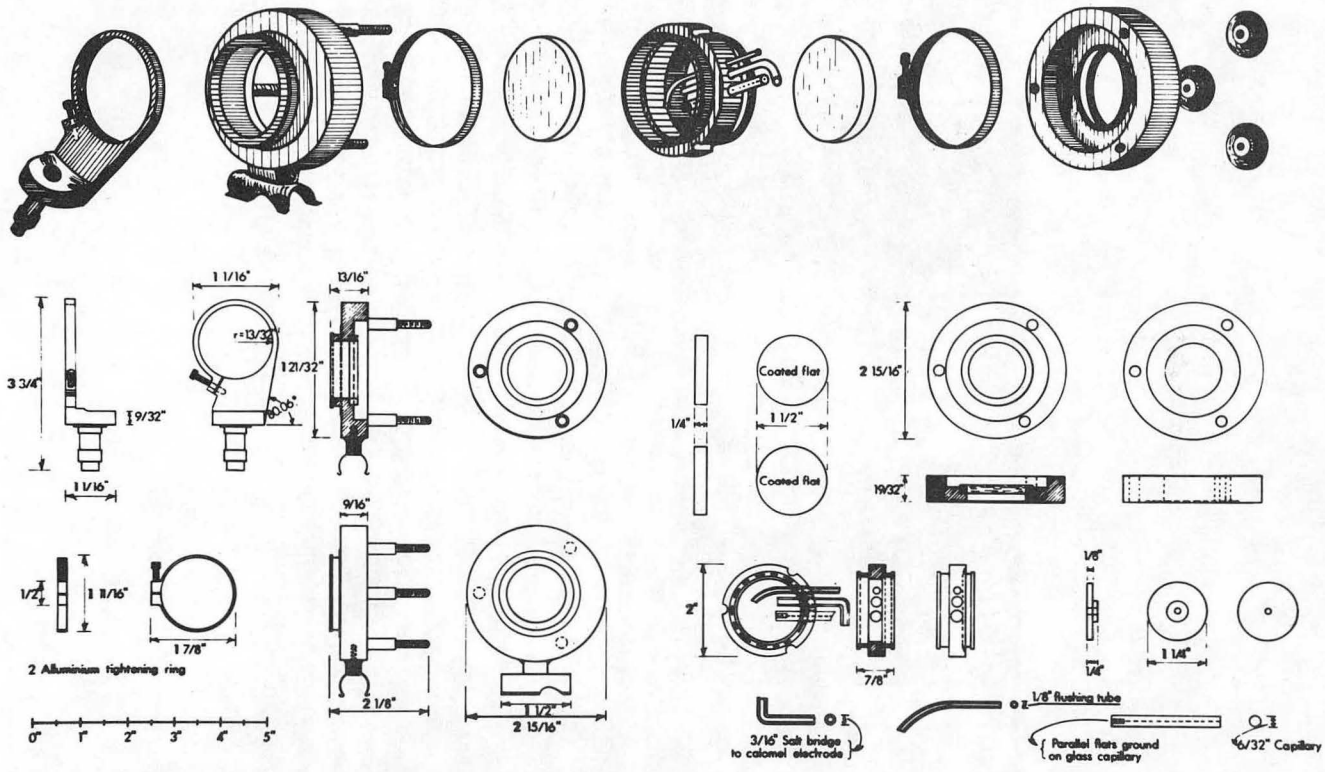

MUB-12630

Fig. VII

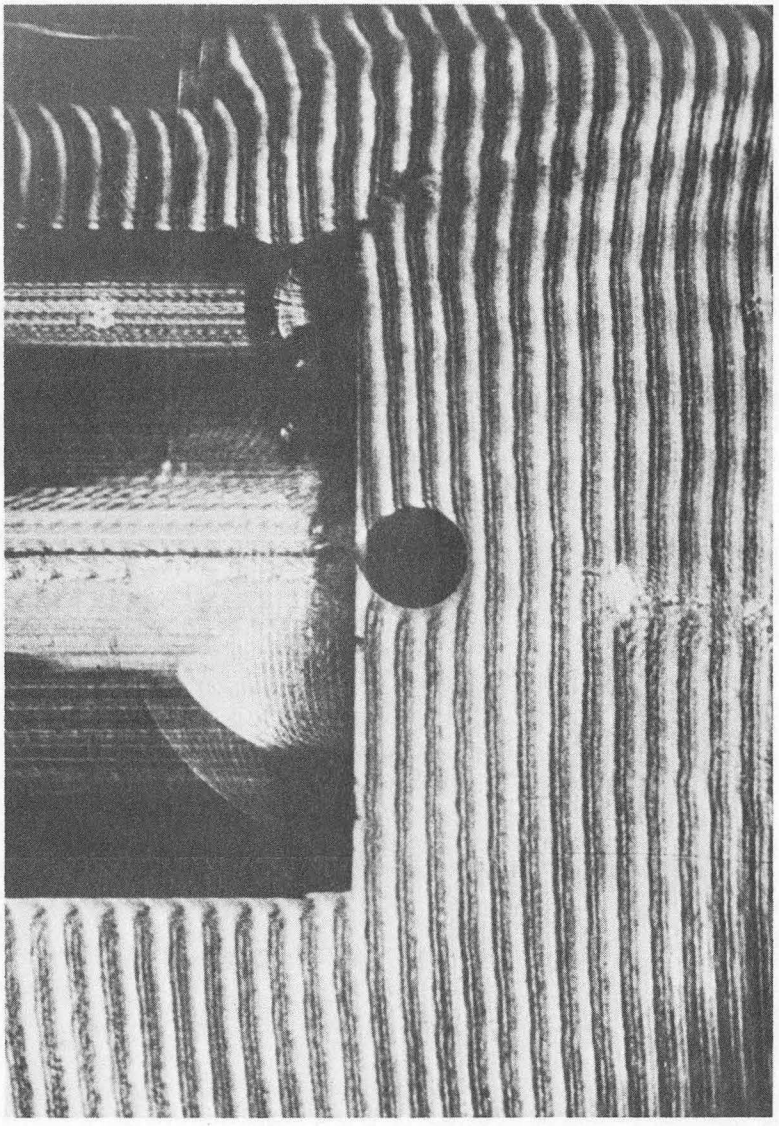

ZN-5743

Fig. VIII

LONG-PATH LASER INTERFEROMETER CELLS FOR USE IN CONDENSED PHASES.

II. Interferometric Cells Other Than Electrodeposition.

By R. N. O'Brien, S. Weiner* and K. S. Spiegler.*

Refractive index is a distinctive property of all phases of all matter and has been used as an analysis tool for many years,[1] but the analysis has been a spot analysis rather than a constantly measured variable in a physical process or a chemical reaction. The transport of solute in the growth of a crystal from a saturated solution was observed interferometrically by Berg[2] in a fairly thin cell. Cells are now presented in which the physical processes of gas dissolution in liquids, the conduction of heat in transparent liquids and the electrodialysis of sea water can be observed continuously. It is also thought that the formation of hydrocarbon hydrates[3] (clathration compounds) has been observed and there appears to be no reason why the kinetics of chemical reactions with low enthalpies of reaction such as the hydrolysis of an ester could not be studied this way. The addition of a thermocouple and prior knowledge of the thermal coefficients of refractive index of all reactants would permit calculation

*Present address: Sea Water Conversion Laboratory, University of California, Richmond, California.

of reaction rates even when the complication of moderate enthalpies of reaction were encountered.

An Electrodialysis Cell

Some problems such as concentration polarization at ion exchange membranes in electrodialysis can more easily be investigated when they can be observed directly. A cell was built (Figure I) in which an anion and a cation exchange membrane were set into a teflon cell case which was machined to admit an Ag/AgCl electrode behind each membrane and sea water in front of them. The remainder of the cell, clamps, thermostat, etc., were identical to the DME cell in paper I but 3.25 mm thick instead of 7.65 mm. The fringes were arranged perpendicular to the surface of the membranes and at constant c.d. the build-up of concentration contours was recorded with a 16 mm motion picture camera. Figure II is an interferogram from a 16 mm frame in which San Francisco Bay water, filtered and diluted to 1/10 normal concentration is being electrodialized at 3.4 ma/cm (Figure II b). Experiments were performed with no flow of water occurring and at desired flow rates. The cell is being redesigned to minimize turbulence introduced by the shape of the flow channels.

Gas-Liquid Solubility and Diffusivity Cell

A gas-tight cell was designed (Figure III) to study the effect of dissolving gases in liquids. The cell was originally planned to obtain refractive index data for gases in liquids so that the generation of gas at electrodes could be studied interferometrically. It was found (Figure IV) that the fringe perturbation was for all gases initially in such a direction as to indicate a dilation of the liquid on dissolution of the gas. In the case of hydrocarbons that form clathrates[3] as propane or isobutane (Figure IV), a later densification occurs and this is thought to be evidence for clathration. The stoichiometric unit is 17 $H_2O \cdot 3M$ (where M is a suitable molecule such as propane) and the unit cell is 17 Å on a side consisting of 136 water molecules which would suggest a slower process than diffusion of the gas into the liquid.[3]

A wide variety of gases and some interesting water solutions have been used and the results will soon be reported. The interferogram shown was obtained with a 16 mm motion picture camera using a prototype of the cell shown. The principal difference was that the cell body was made of teflon and at the highest pressures (about 10 atmospheres) the cell expanded and had to be calibrated so that the expansion could be corrected for.

Thermal Conductivity Cell

A cell (Figure V) was designed specifically to measure the thermal conductivity of transparent liquids. The original use was intended to allay criticism of interferograms taken in electrochemical cells where thermal effects are known to occur at electrodes at high current densities. Figure VI is an interferogram from a 16 mm motion picture frame showing the result of injecting refrigerated water into a cell which was at room temperature containing copper blocks whose thermal capacity was much larger than the water. As the water warms up, its refractive index change can be used to calculate its temperature change. The cell used was a prototype of that shown in Figure V. Associated liquids show anomalous refractive index changes with temperature and water in particular does not show a linear dependence between the two variables.[4]

The cell shown is a modification which more completely satisfies the condition for one dimensional heat flow than the prototype and has extremely high thermal capacity. Each side can be thermostated separately and hence it can be used to observe transient and steady state thermal conductivity.

It is intended to study solutions of associated electrolytes in various solvents and associated and unassociated pure liquids.

Acknowledgements

Some of the work in this part was done at the University of Alberta with support from the National Research Council of Canada and the Defence Research Board of Canada on DRB Grant 5401-04. One of us (R. N. O'Brien) was a Visiting Scholar at the University of California, Berkeley and was supported by IMRD, LRL where most of the work was done. The Sea Water Conversion Laboratory also contributed to the support of the work. To all of these agencies the authors wish to express their gratitude.

This work was partially supported by the United States Atomic Energy Commission.

References

1. S. Glasstone, Textbook of Physical Chemistry, 2nd Ed., Van Nostrand, New York (1946). pp. 528-532.

2. W. F. Berg, Discussions Faraday Soc. 1, 44 (1947).

3. M. Hagan, Clathrate Inclusion Compounds, Reinhold Publishing Corp., New York (1962). p. 59.

4. R. N. O'Brien, The Refractive Index of Zinc and Copper Sulfate in Various Solutions and Some Other Refractive Indices at Gas Laser and Sodium Vapor Frequencies, submitted to J. of Chem. and Eng. Data.

FIGURE CAPTIONS (Paper 2)

Figure I — Detail of the Electrodialysis Cell. The core shown fits into a teflon body similar to the Dropping Mercury Electrode cell in Paper 1.

Figure II — Interferograms showing concentration changes around ion exchange membranes. Striated areas are San Francisco Bay water (diluted 10:1, 1636 ppm). Vertical black solid shadows are anion-exchange membrane (right) and cation-exchange membrane (left). Vertical channel 1.58 mm, horizontal 3.17 mm. Solution stationary . Frame (a) is before passage of current, (b) is at quasi-steady-state polarization during passage of positive current (right to left) of 3.4 mA/cm^2 through silver-silver chloride electrodes place outside the camera's field of view.

Figure III — Detail of Gas-Liquid Diffusion Cell.

Figure IV — Two Interferograms of Propane Dissolving in water. The top frame taken $\frac{1}{4}$ second after about 120 pounds per square inch above one atmosphere was applied and the bottom one 7/12 of a second after the pressure application at 24°C. The refractive index gradient has changed sign in 1/3 of a second at the gas-liquid interface (the curved horizontal line crossing the centre of each frame).

Figure V — Detail of the Thermal Conductivity Cell.

Figure VI — Thermal Conductivity Interferogram. Refrigerated water (5.2°C) was injected into the cell which was at 22°C. The interferogram shows the change of refractive index with temperature as heat flows from the copper block walls into the water. Time elapsed from injection, $\frac{1}{4}$ second, thermal equilibrium required $\sim$1 second. Distance across the channel is 0.43 mm.

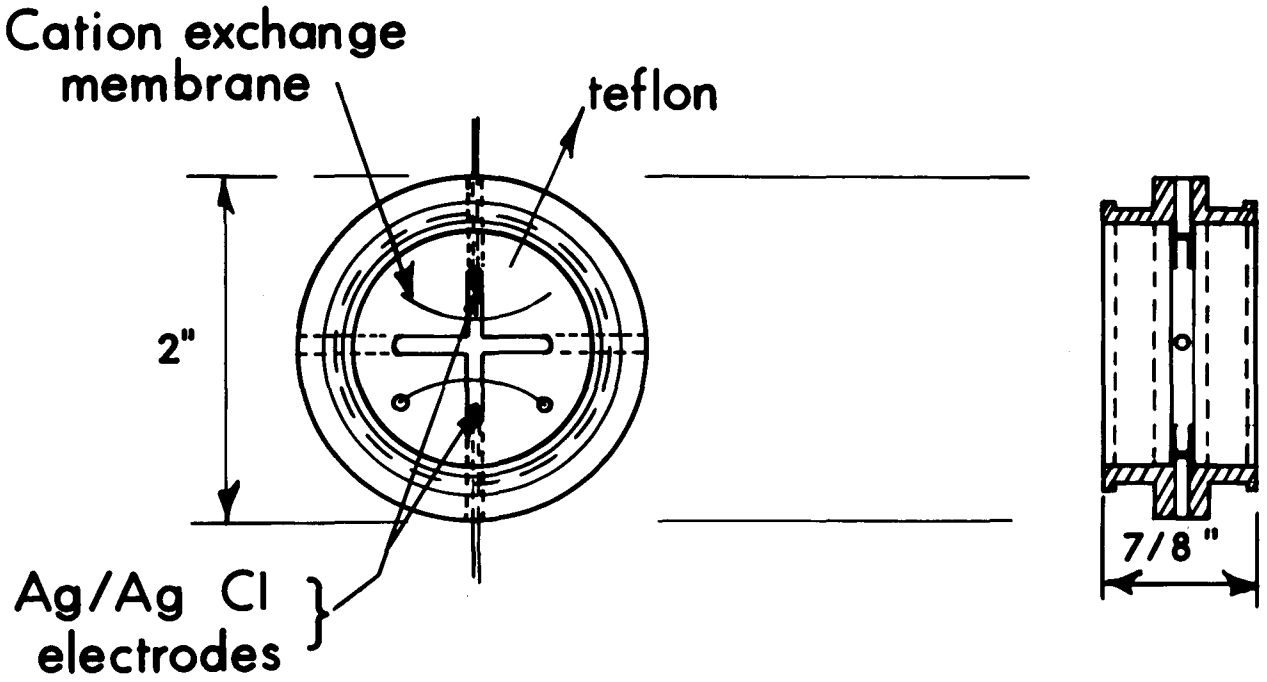

MUB-12631

Fig. I

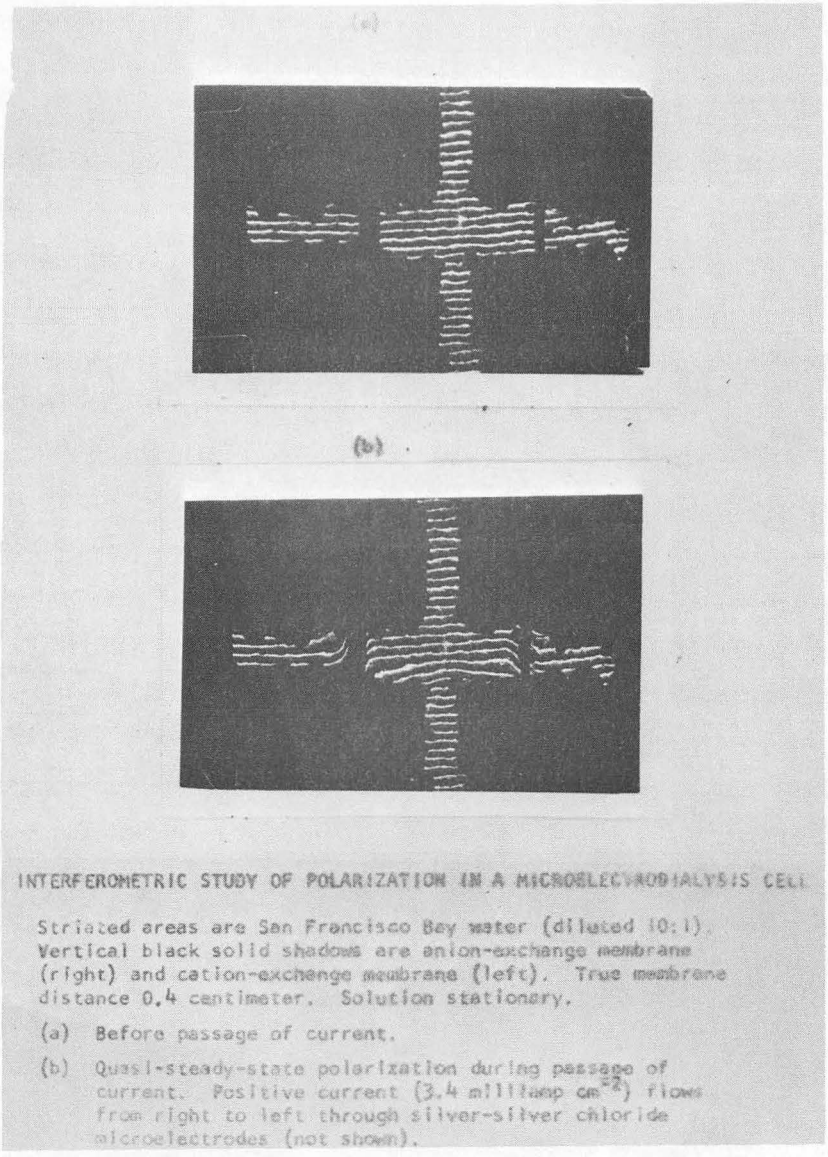

INTERFEROMETRIC STUDY OF POLARIZATION IN A MICROELECTRODIALYSIS CELL

Striated areas are San Francisco Bay water (diluted 10:1). Vertical black solid shadows are anion-exchange membrane (right) and cation-exchange membrane (left). True membrane distance 0.4 centimeter. Solution stationary.

(a) Before passage of current.

(b) Quasi-steady-state polarization during passage of current. Positive current (3.4 milliamp cm^{-2}) flows from right to left through silver-silver chloride microelectrodes (not shown).

ZN-5742

Fig. II

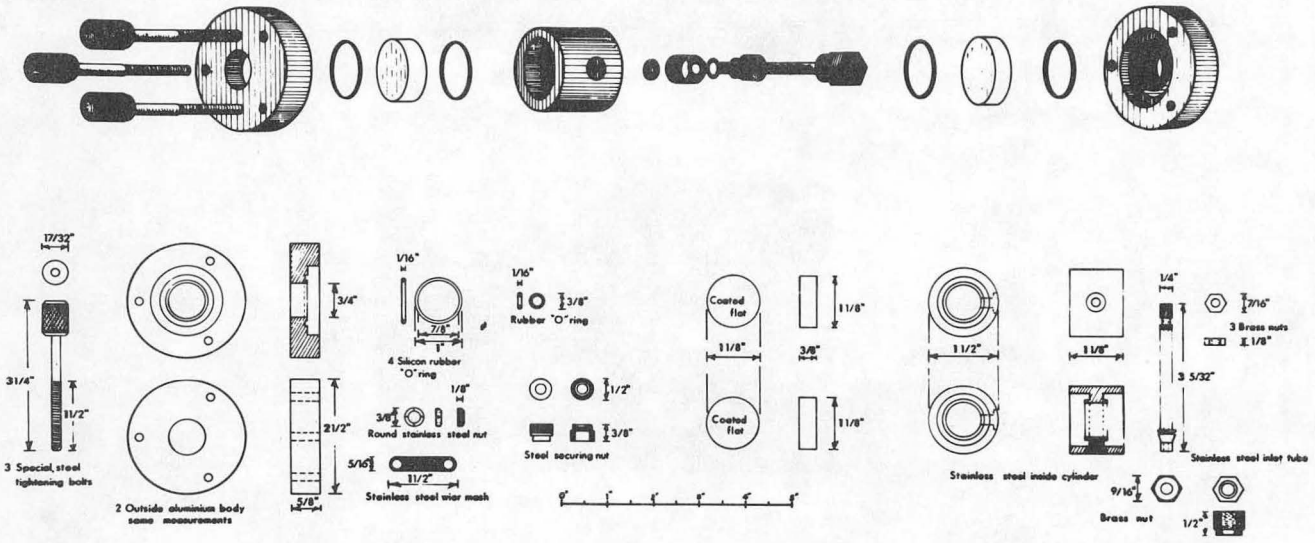

MUB-12632

Fig. III

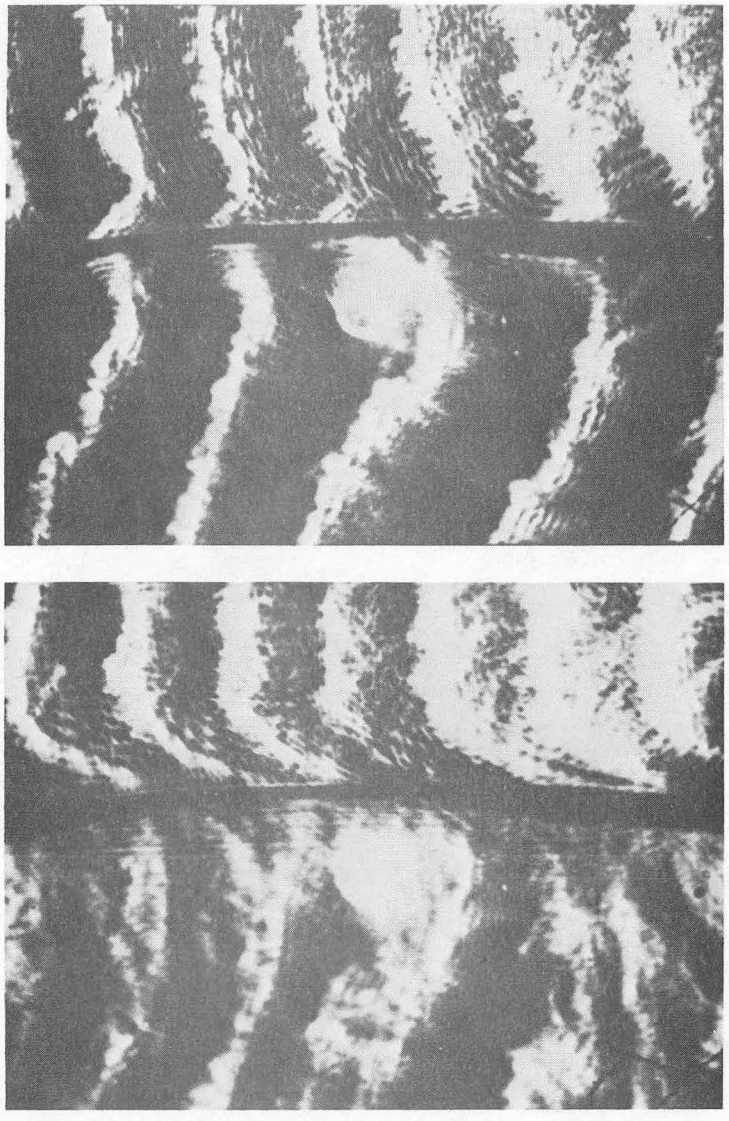

ZN-5739

Fig. IV

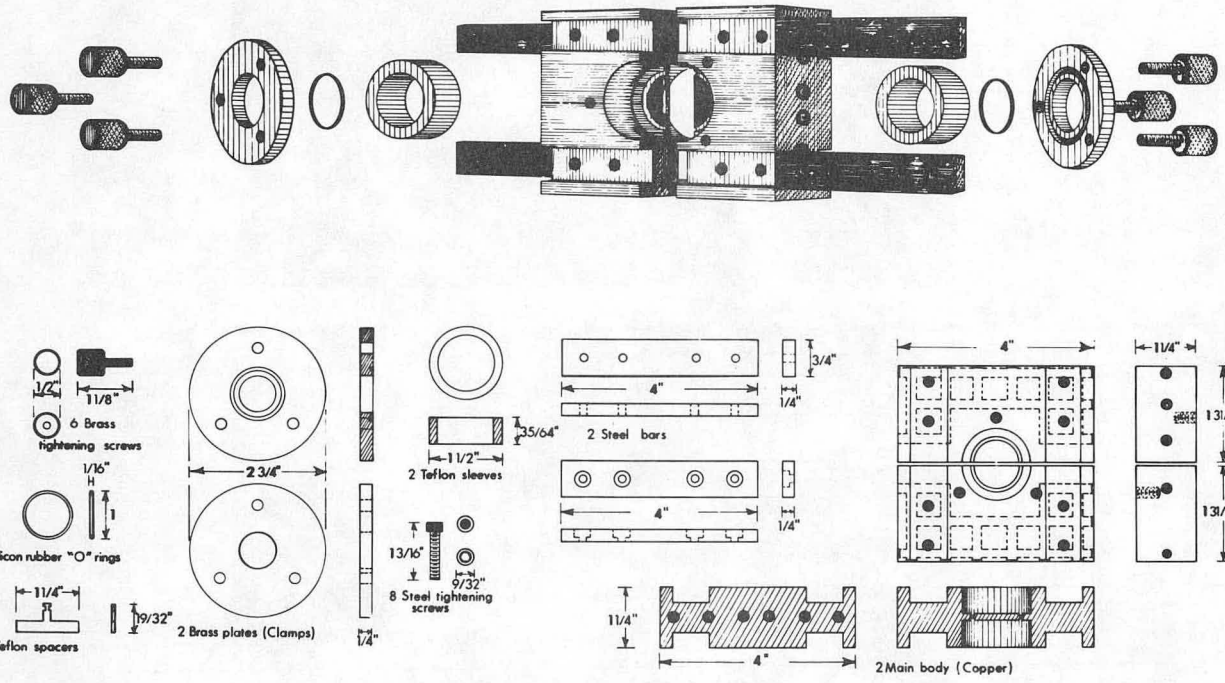

MUB-12633

Fig. V

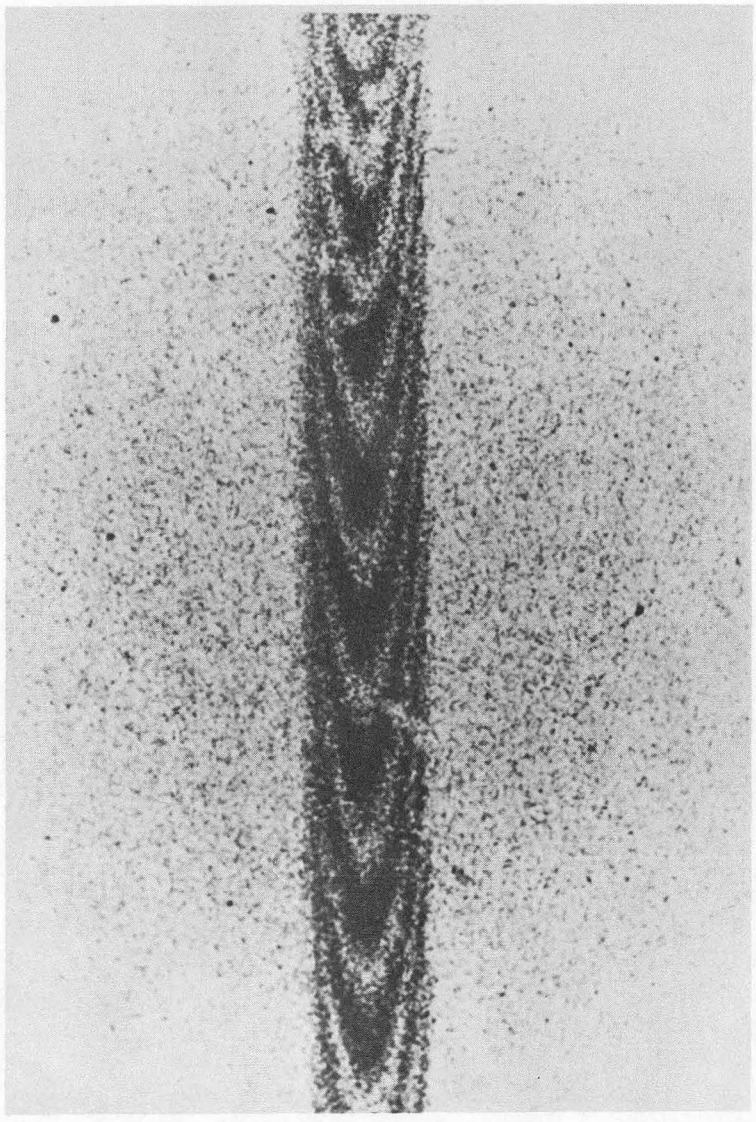

ZN - 5744

Fig. VI

(1) Present address, Department of Chemistry, University of Alberta, Edmonton, Alberta, Canada to whom inquiries should be directed.

(2) Present address, Chemical Laboratory, University of Pennsylvania, Philadelphia, Pennsylvania.

(3) Present address, IMRD, Lawrence Radiation Laboratory, University of California, Berkeley, California.

(4) Present address, Mineral Engineering Department, University of British Columbia, Vancouver, British Columbia.

This report was prepared as an account of Government sponsored work. Neither the United States, nor the Commission, nor any person acting on behalf of the Commission:

A. Makes any warranty or representation, expressed or implied, with respect to the accuracy, completeness, or usefulness of the information contained in this report, or that the use of any information, apparatus, method, or process disclosed in this report may not infringe privately owned rights; or

B. Assumes any liabilities with respect to the use of, or for damages resulting from the use of any information, apparatus, method, or process disclosed in this report.

As used in the above, "person acting on behalf of the Commission" includes any employee or contractor of the Commission, or employee of such contractor, to the extent that such employee or contractor of the Commission, or employee of such contractor prepares, disseminates, or provides access to, any information pursuant to his employment or contract with the Commission, or his employment with such contractor.